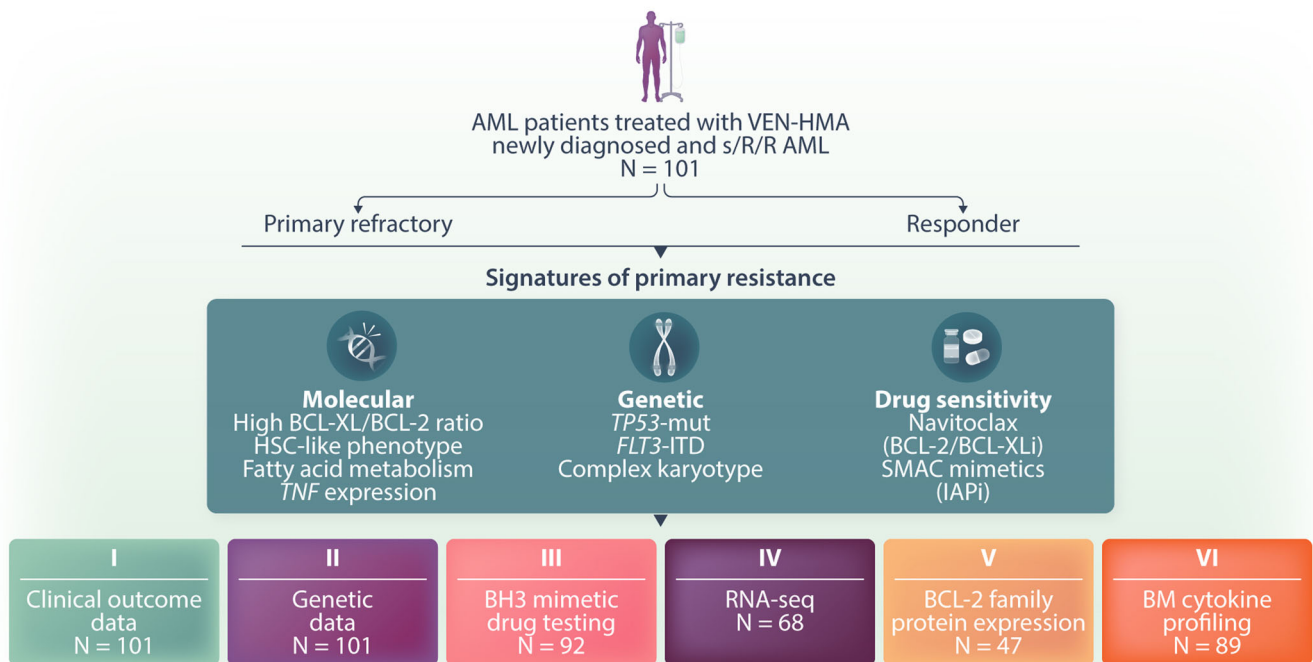


Drivers of clinical resistance to venetoclax and hypomethylating agents in acute myeloid leukemia and strategies for improving efficacy

Ida Vänttinen^{1,2}  | Joseph Saad^{1,2}  | Tanja Ruokoranta^{1,3}  | Sari Kytölä³ |
 Guangrong Qin⁴  | Bahar Tercan⁴ | Pia Ettala⁵ | Anu Partanen⁶  |
 Marja Pyörälä⁶  | Johanna Rimpiläinen⁷ | Timo Siitonen⁸ | Mikko Manninen⁹  |
 Peter J. M. Valk¹⁰  | Gerwin Huls¹¹  | Vésteinn Thorsson⁴  |
 Caroline A. Heckman^{1,2}  | Mika Kontro^{1,2,3,12,^}  | Heikki Kuusanmäki^{1,2,^} 

Graphical Abstract



Drivers of clinical resistance to venetoclax and hypomethylating agents in acute myeloid leukemia and strategies for improving efficacy

Ida Vänttinen^{1,2}  | Joseph Saad^{1,2}  | Tanja Ruokoranta^{1,3}  | Sari Kytölä³ |
Guangrong Qin⁴  | Bahar Tercan⁴ | Pia Ettala⁵ | Anu Partanen⁶  |
Marja Pyörälä⁶  | Johanna Rimpiläinen⁷ | Timo Siitonen⁸ | Mikko Manninen⁹  |
Peter J. M. Valk¹⁰  | Gerwin Huls¹¹  | Vésteinn Thorsson⁴  |
Caroline A. Heckman^{1,2}  | Mika Kontro^{1,2,3,12,^}  | Heikki Kuusanmäki^{1,2,^} 

Correspondence: Mika Kontro (mika.kontro@helsinki.fi) and Heikki Kuusanmäki (heikki.kuusanmaki@helsinki.fi)

ABSTRACT

The B-cell lymphoma 2 (BCL-2) inhibitor venetoclax (VEN) in combination with hypomethylating agents (HMAs) has improved treatment outcomes for acute myeloid leukemia (AML) patients unfit for intensive chemotherapy and is increasingly used in the relapsed/refractory setting. However, primary resistance remains a significant challenge, affecting 20%–35% of treatment-naïve and around 50% of previously treated AML patients. To investigate the mechanisms driving primary resistance to VEN–HMA therapy, we analyzed genetic, transcriptomic, BCL-2 family protein expression, and ex vivo drug sensitivity data from 101 AML patients and correlated these profiles with clinical outcomes to VEN–HMA. Our study found that blasts from refractory patients exhibit an elevated BCL-XL/BCL-2 protein expression ratio, an immature CD34⁺CD38⁻ phenotype, and frequent *TP53* mutations. Consistent with the high ratio of BCL-XL/BCL-2, resistant samples showed increased ex vivo sensitivity to the dual BCL-2/BCL-XL inhibitor navitoclax. In addition, SMAC mimetics were effective in refractory blasts, which correlated with high *TNF* gene expression in these cells. Ex vivo treatment with the combination of navitoclax and SMAC mimetics further enhanced the eradication of VEN–HMA refractory blasts, although toxicity was also observed in healthy CD34⁺ cells. In conclusion, our integrative analysis identifies molecular signatures associated with primary VEN–HMA resistance and highlights BCL-2/BCL-XL inhibition and SMAC mimetics as therapeutic strategies to target resistance.

INTRODUCTION

Acute myeloid leukemia (AML) is an aggressive hematologic malignancy associated with poor outcomes, particularly in elderly patients and those with high-risk disease.¹ Venetoclax (VEN), a selective B-cell

lymphoma 2 (BCL-2) inhibitor in combination with the hypomethylating agents (HMAs) azacitidine (AZA) or decitabine, has emerged as a standard frontline treatment for previously untreated AML patients unfit for intensive chemotherapy.² Approximately 60–75% of these patients achieve complete remission (CR) or CR with incomplete

¹Institute for Molecular Medicine Finland (FIMM), HiLIFE, University of Helsinki, Helsinki, Finland

²ICAN Digital Precision Cancer Medicine Flagship, Helsinki, Finland

³Department of Hematology, Helsinki University Hospital Comprehensive Cancer Center, Helsinki, Finland

⁴Institute for Systems Biology (ISB), Seattle, Washington, United States

⁵Department of Clinical Hematology and Stem Cell Transplant Unit, Turku University Hospital, Turku, Finland

⁶Department of Medicine, Kuopio University Hospital, Kuopio, Finland

⁷Department of Internal Medicine, Tampere University Hospital, Tampere, Finland

⁸Cancer Center, Oulu University Hospital and Research Unit of Biomedicine and Internal Medicine, University of Oulu, Oulu, Finland

⁹Orton Orthopedic Hospital, Helsinki, Finland

¹⁰Department of Hematology, Erasmus MC Cancer Institute, University Medical Center Rotterdam, Rotterdam, The Netherlands

¹¹Department of Hematology, University Medical Center Groningen, University of Groningen, Groningen, The Netherlands

¹²Foundation for the Finnish Cancer Institute, Helsinki, Finland

[^]Shared corresponding authorship.

This is an open access article under the terms of the [Creative Commons Attribution-NonCommercial-NoDerivs](https://creativecommons.org/licenses/by-nc-nd/4.0/) License, which permits use and distribution in any medium, provided the original work is properly cited, the use is non-commercial and no modifications or adaptations are made.

© 2026 The Author(s). *HemaSphere* published by John Wiley & Sons Ltd on behalf of European Hematology Association.

hematologic recovery (CRI) following VEN-HMA, with a median overall survival (OS) of 15 months.^{2,3} In addition, VEN-based regimens are increasingly administered to patients with relapsed/refractory (R/R) disease or previously treated secondary AML (sAML), although only about half of these patients achieve a response, with a median OS of 4–8 months.^{4–6} Therefore, a more comprehensive understanding of the underlying mechanisms mediating VEN-HMA resistance is needed for improving patient outcomes and advancing AML treatment.

Genetic predictors of response and resistance to VEN-HMA are relatively well characterized: *IDH2* and *NPM1* mutations are generally associated with favorable outcomes, while *FLT3-ITD*, *PTPN11*, *KRAS*, and particularly *TP53* mutations correlate with poor outcomes.^{2,7–9} More recently, a 4-gene molecular prognostic risk signature (mPRS, ELN 2024) based on *FLT3-ITD*, *NRAS*, *KRAS*, or *TP53* mutational status outperformed the European LeukemiaNet (ELN) 2022 risk classification in predicting treatment outcomes for newly diagnosed (ND) AML patients receiving VEN-HMA therapy.^{10–12}

Molecular mechanisms of VEN-HMA resistance have been shown to include a shift in dependence from BCL-2 to other anti-apoptotic BCL-2 family members, such as BCL-XL and MCL-1,^{13–15} as well as metabolic reprogramming of leukemic stem cells (LSCs) toward fatty acid utilization.¹⁶ Moreover, the bone marrow (BM) microenvironment and inflammatory cytokines, such as interferon (IFN), have been suggested to protect LSCs from BCL-2 inhibition.^{17,18}

Emerging evidence also indicates that the differentiation stage of AML blasts influences venetoclax sensitivity and clinical responses. Studies involving ex vivo drug testing have shown that monocytic AML samples are resistant to venetoclax^{13,19–22} and demonstrate increased dependence on MCL-1,²³ whereas erythroid differentiation is associated with BCL-XL upregulation.²⁴ While the clinical impact of monocytic differentiation on resistance has been debated,^{13,23,25–29} a recent study of 451 patients demonstrated inferior survival in patients with monocytic AML, except in patients harboring *NPM1* mutations whose outcomes remained favorable irrespective of the disease subtype.³⁰

Despite several proposed mechanisms, only a few studies have linked molecular signatures of patient-derived blasts—beyond genetic alterations—to clinical responses.^{13,31,32} Our prospective VenEx clinical trial (NCT04267081) demonstrated that ex vivo venetoclax sensitivity of blasts measured by flow cytometry predicts response to VEN-AZA.^{33,34} In the present study, we extend these findings by correlating RNA-seq, BCL-2 family protein expression, and BH3 mimetic drug sensitivity data from patient-derived AML blasts with clinical outcomes to VEN-HMA.

METHODS

A more detailed description of the methods is available in Supporting Information S1.

AML patient samples and treatment

BM ($n = 107$) or peripheral blood (PB, $n = 6$) aspirates were collected from 113 adult AML patients screened for the VenEx trial (NCT04267081) or treated at Helsinki University Central Hospital (HUCH), Finland. Of the 113 patients, 101 received VEN-HMA (azacitidine $n = 100$; decitabine $n = 1$) in 28-day cycles of azacitidine plus venetoclax, with venetoclax shortened to 14–21 days in responders. Patients without a response after three cycles were classified as refractory.^{33,34} The remaining 12 patients did not receive VEN-HMA due to ex vivo venetoclax resistance, as outlined in the trial protocol.^{33,34} BM samples from 28 patients with *TP53*-mutated AML were retrieved outside the study from the Finnish Hematology Registry

and Clinical Biobank (FHRB, $n = 17$) and the HOVON Biobank ($n = 11$). Two healthy BM samples were obtained from HUCH to assess drug toxicity. All samples were collected after informed consent in accordance with the Declaration of Helsinki under ethical permits (HUS/3235/2019, HUS/6338/2023, HUS/395/2018).

Sample processing

Mononuclear cells (MNCs) from AML patients were isolated by gradient centrifugation (Ficoll-Paque Plus, Cytiva, #17144003) and resuspended in conditioned medium (CM) (RPMI-1640, Lonza, #BE12-167F, 10% h.i. fetal bovine serum [FBS], 2 mM L-glutamine, 100 units/mL penicillin, 100 μ g/mL streptomycin, and 12.5% HS-5 CM) for ex vivo drug sensitivity testing. CM was prepared as previously described.³³ The remaining cells were cryopreserved in 95% FBS with 5% dimethyl sulfoxide (DMSO) for subsequent analyses.

Flow cytometry-based drug sensitivity assay

Freshly isolated or viably frozen MNCs were seeded on 96-well plates with increasing concentrations of BH3 mimetics or SMAC mimetics (drug panel and concentrations in Supporting Information: Table S1). After 48 h of drug treatment at 37°C, cells were stained with cell surface antibodies and then with viability dyes (antibodies listed in Supporting Information: Table S2). Cells were analyzed using the iQue Screener Plus flow cytometer (Sartorius, Germany) and gated as shown in Supporting Information: Figure S1. The absolute viable blast count was normalized to DMSO controls, followed by dose–response analysis. A drug sensitivity score (DSS) was calculated based on the area above the viability curve, as previously described,³⁵ to quantify drug efficacy.

CellTiter-Glo drug combination assay

MNCs from AML patients were seeded on 384-well plates containing six unique combinations of BH3 mimetics and SMAC mimetics arranged in 8 \times 8 drug matrices (details in Supporting Information: Table S3). After 48 h, viability was assessed using the CellTiter-Glo (CTG) 2.0 Luminescent cell viability assay (Promega, #G942C). Synergy, the most synergistic area, and potency scores were calculated for each drug combination using web-based tools (<https://syntoxprofiler.fimm.fi>, <https://synergyfinder.fimm.fi>).^{36,37} Potency scores were quantified based on the normalized volume under dose–response surface, and synergy effect was derived using the zero-interaction potency (ZIP) model.³⁸

RNA-sequencing of isolated blasts

Blasts were isolated from AML patient samples using CD34 (StemCell Technologies, #17856), CD117 (Miltenyi Biotec, #130-091-332), or CD33 (Miltenyi Biotec, #130-045-501) immunomagnetic beads. Enrichment beads were selected based on available immunophenotyping data of blast cells. CD34 ($n = 54$) was primarily used, followed by CD117 ($n = 18$) or CD33 ($n = 2$) in cases where CD34 or CD117 expression was negative. RNA was extracted according to the AllPrep DNA/RNA/miRNA Universal Kit (Qiagen, #80224), sequenced on the Illumina NovaSeq system (Illumina, San Diego, CA, USA), and processed in the Illumina DRAGEN v4.2 pipeline. Raw RNA counts were normalized and transformed into log₂ counts per million (CPM) values using edgeR. Before downstream analyses, lowly expressed genes were filtered out, retaining only those with CPM ≥ 1 in at least 10% of the samples.

Anti-apoptotic BCL-2 family protein quantification with flow cytometry

MNCs from AML patients were first stained with Zombie NIR viability dye and then with cell surface antibodies (antibodies listed in Supporting Information: Table S4). After the staining, cells were washed, fixed, and permeabilized according to the manufacturer's guidelines (Cytofix/Cytoperm Kit, BD Biosciences, #554714). Consecutively, cells were stained with intracellular antibodies (antibodies listed in Supporting Information: Table S4). Median fluorescence intensity (MFI) of each intracellular marker was measured using flow cytometry (iQue3, Sartorius, Germany) from AML blasts gated as shown in Supporting Information: Figure S1. MFIs were normalized to a reference sample included in each batch and converted to relative values by dividing each marker by the cohort median. Normalized relative values were then used to calculate protein expression ratios.

Cytokine profiling

Fresh BM or PB aspirates from AML patients and BM from healthy individuals ($n = 8$) undergoing hip replacement surgery (median age 64 years, range 50–78 years) were processed by centrifugation at $1300 \times g$ for 10 min. The isolated plasma samples were stored at -80°C , and the concentrations of 45 inflammatory cytokines were measured using the Olink Target 48 platform (Olink®, Uppsala, Sweden). Normalized protein expression (NPX) was used in downstream analyses.

Statistical analyses

Appropriate statistical methods were applied according to data distribution and sample size. Comparative analyses were performed using *t*-test, Wilcoxon rank-sum test, or analysis of variance (ANOVA), with *P*-values adjusted for multiple comparisons using false discovery rate (FDR). Univariate logistic regression was used to detect genetic associations with primary response to VEN-HMA, and Cox proportional regression with hazard ratio estimation was applied for survival analyses. All statistical analyses and data visualizations were performed using the R software version 4.1.2 or Prism 10.

RESULTS

AML patient cohort and molecular profiling

The study included 101 patients with ND treatment-naïve ($n = 50$, 50%), previously treated R/R ($n = 36$, 36%), or secondary ($n = 15$, 15%) AML (Figure 1A). All patients received VEN-HMA, of whom 23 had refractory disease (RD), 62 achieved remission (CR/CRi/CRh), and 14 reached morphologic leukemia-free state (MLFS). Two patients were excluded from response evaluation due to early death. For subsequent data analyses, the 23 RD patients were categorized as refractory, and those achieving CR/CRi/CRh or MLFS were considered responsive ($n = 76$) (Figure 1A). Patients with MLFS were classified as responsive as most of their blasts were cleared rather than persisted following VEN-HMA treatment. Patient characteristics and treatment outcomes are detailed in Supporting Information: Table S5.

The cohort was profiled using ex vivo drug sensitivity testing with BH3 mimetics ($n = 92$), RNA-sequencing ($n = 68$), BCL-2 family protein quantification ($n = 47$), and BM cytokine analysis ($n = 89$) (Figure 1B). To ensure leukemia-specific measurements in heterogeneous AML samples, analyses were focused on blasts (mainly CD34⁺ or CD117⁺). An overview of the patient-level clinical and genetic features, along

with available molecular and drug sensitivity data, is presented in Figure 1C and detailed in Supporting Information: Table S6.

In addition to the VEN-HMA-treated patient cohort, 12 VenEx trial participants with R/R/sAML, whose blasts were venetoclax-resistant in ex vivo drug testing, were profiled. Per trial protocol*, they did not receive VEN-HMA^{33,34} and were only included in analyses not linked to clinical outcome. Venetoclax resistance was defined as a DSS < 10.7, based on a receiver operating characteristic (ROC) curve analysis correlating ex vivo drug sensitivity with clinical response³⁴ (Figure 1A).

Ex vivo drug sensitivity testing reveals BCL-XL/BCL-2 dependence in VEN-HMA refractory blasts

To functionally test the dependency of AML blasts on anti-apoptotic BCL-2 family members, we analyzed the ex vivo drug sensitivity of blasts from 92 AML patients to four BH3 mimetics (Figure 2A). The drug sensitivity scores differed significantly between blasts from VEN-HMA refractory ($n = 21$) and responsive ($n = 71$) patients (Figure 2B) but not between disease stages (Supporting Information: Figure S2A,B). As previously demonstrated in the VenEx trial,³³ blasts from VEN-HMA responsive patients had significantly higher venetoclax sensitivity scores (median DSS responsive 25.4 vs. refractory 8.4, $P < 0.00001$), which also correlated with prolonged OS (Supporting Information: Figure S2C). In blasts from VEN-HMA refractory patients, the dual BCL-2/BCL-XL inhibitor navitoclax (NAV) was significantly more effective than venetoclax (median DSS NAV 17.3 vs. VEN 8.4, $P < 0.0001$), whereas no such benefit was observed in blasts from responsive patients (Figure 2B). Similarly, the BCL-XL inhibitor A-1331852 showed increased efficacy in VEN-HMA refractory blasts when compared to those from responsive patients (median DSS 12.1 vs. 6.7, $P < 0.01$). The MCL-1 inhibitor S-63845, however, demonstrated limited activity in both groups (median DSS 5.6 vs. 5.8) (Figure 2B).

We next focused on the clinically refractory cohort ($n = 21$) to identify potential patient subgroups with alternative BCL-2 family dependencies (Figure 2C). Samples were ranked by their ex vivo venetoclax sensitivity, and samples from five patients displayed clear venetoclax sensitivity (DSS 17–33) despite clinical refractoriness. No definitive explanation was identified for these five patients; however, all had R/R/sAML, and 4/5 were previously exposed to HMA, though this association was not statistically significant (Supporting Information: Table S7). Among the remaining 16 ex vivo-resistant and in vivo refractory patients, several showed increased ex vivo sensitivity to navitoclax and a subset to selective BCL-XL inhibition (Figure 2C,D). These findings indicate that BCL-XL or BCL-2/BCL-XL co-dependence may underlie venetoclax resistance in a subset of refractory patients.

Distinct transcriptomic features underlie resistance to VEN-HMA

To investigate the transcriptional programs underlying VEN-HMA resistance, we used RNA-seq data of blasts isolated from 68 AML patient samples (Supporting Information: Figure S3A). Differential gene expression analysis between 15 clinically refractory and 53 clinically responsive patients resulted in 200 significantly deregulated genes (adj. *P*-value < 0.05) (Figure 3A, Supporting Information: Table S8). Among the anti-apoptotic BCL2 family genes, *BCL2L1* (BCL-XL) was overexpressed in blasts from refractory patients, while *BCL2* and *MCL1* were downregulated (Figure 3B). No significant differences were observed in the expression of pro-apoptotic BCL2 family members (Figure 3C). Instead, refractory blasts displayed upregulation of genes linked to standard therapy resistance and stemness, such as *PEAR1* (platelet

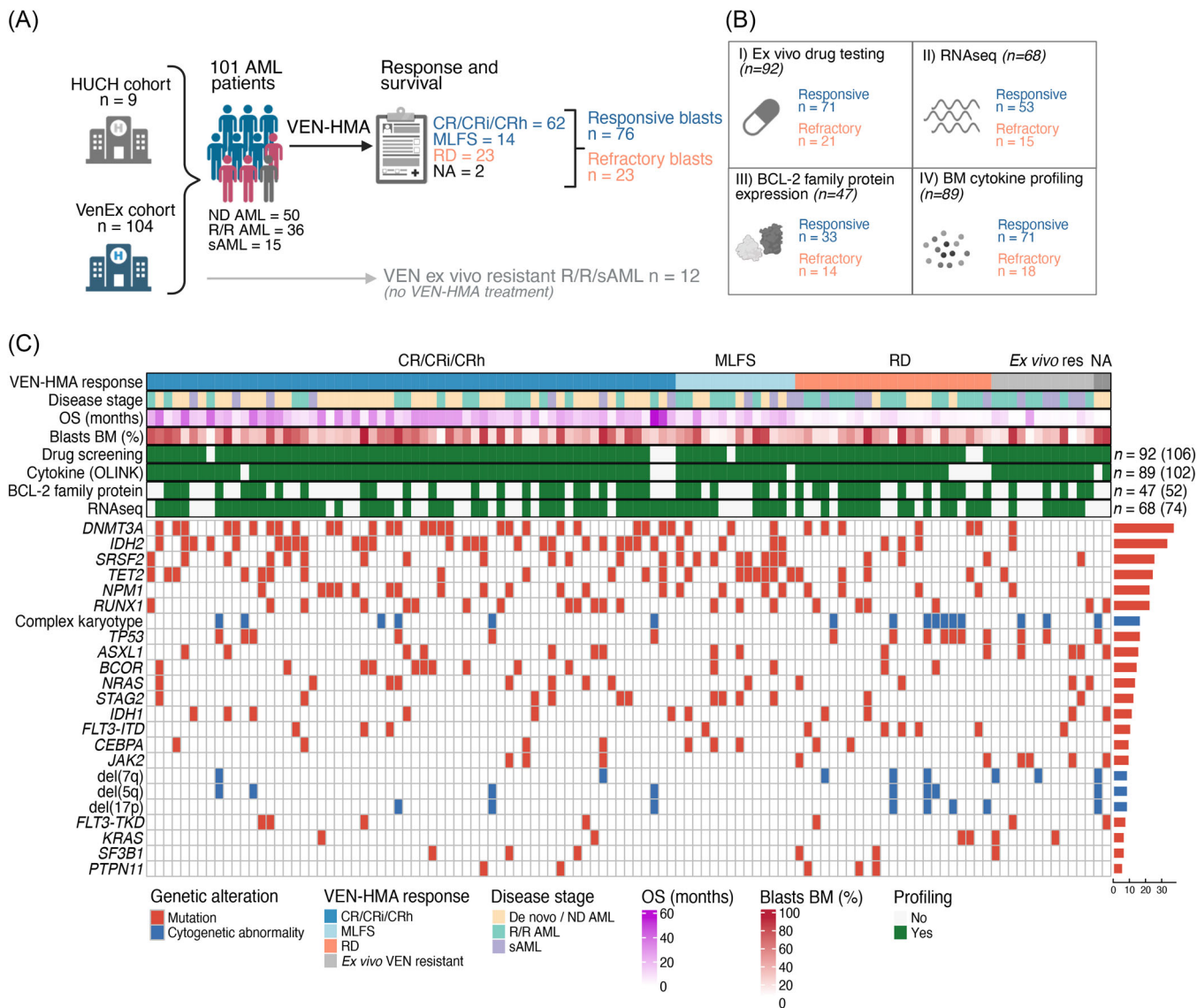


FIGURE 1 Study design and molecular profiling of acute myeloid leukemia (AML) patients before venetoclax (VEN)-hypomethylating agent (HMA) treatment. **(A)** Schematic of the study cohort comprising 101 newly diagnosed and previously treated (relapsed/refractory [R/R]/secondary AML [sAML]) AML patients before VEN-HMA. Clinical outcomes included complete remission (CR)/CR with incomplete hematologic recovery (CRi) ($n = 62$), morphologic leukemia-free state (MLFS) ($n = 14$), and refractory disease (RD) ($n = 23$), resulting in 76 responsive and 23 refractory patients. Twelve VEN ex vivo-resistant R/R/sAML patients who did not receive VEN-HMA were retained in the cohort and included exclusively in analyses not associated with clinical outcomes. **(B)** Molecular and functional profiling methods applied in the study. **(C)** Genomic and clinical features of patients receiving VEN-HMA ($n = 101$) and those defined as ex vivo venetoclax-resistant ($n = 12$) with annotation for available functional and molecular data. Sample sizes are shown for each profiling method, with brackets indicating the included ex vivo VEN-resistant patients. BCL-2, B-cell lymphoma 2; BM, bone marrow; HUCH, Helsinki University Central Hospital; ND, newly diagnosed; OS, overall survival.

receptor)²¹ and *MECOM* (transcription factor),³⁹ as well as *TNF* (proinflammatory cytokine), *CD276* (immune checkpoint inhibitor),⁴⁰ and *PRAME* (tumor-testis antigen)⁴¹ (Figure 3A, Supporting Information: Figure S3B). Importantly, these gene expression patterns remained similar across the ND, R/R, and sAML patient cohorts (Supporting Information: Figure S3B).

To further characterize pathway-level alterations, we performed single-sample gene set variation analysis (ssGSVA)⁴² using the hallmark gene set collection⁴³ from the Molecular Signatures Database (MsigDB).⁴⁴ This analysis revealed enrichment of peroxisome and metabolic pathways (cholesterol and heme) in blasts from VEN-HMA refractory patients (Figure 3D, Supporting Information: Table S9). Given the role of peroxisomes in fatty acid catabolism, these findings suggest enhanced fatty acid utilization in refractory blasts, consistent with a prior report.¹⁶

To reveal cell type-specific associations with primary resistance, we computed gene expression scores for six distinct myeloid cell populations using previously curated single-cell RNA-seq-derived gene sets.⁴⁵ Blasts from responsive patients showed an increase in granulocyte-monocyte progenitor (GMP)-like gene expression ($P = 0.05$), whereas refractory blasts showed a trend toward higher hematopoietic stem cell (HSC)-like scores ($P = 0.1$) (Figure 3E). Consistent with the observed trend between the HSC-like gene signature and VEN-HMA resistance, a 17-gene leukemic stem cell signature score (LSC17)⁴⁶ was also elevated in blasts from refractory patients ($P < 0.05$) (Supporting Information: Figure S3C). Notably, these cell type-specific signatures correlated with *BCL2* family gene expression. Elevated *BCL2L1* (*BCL-XL*) levels were associated with higher HSC-like signature ($R = 0.27$, $P < 0.05$), whereas GMP-like scores correlated with lower *BCL2L1* expression ($R = -0.29$, $P < 0.05$). In contrast,

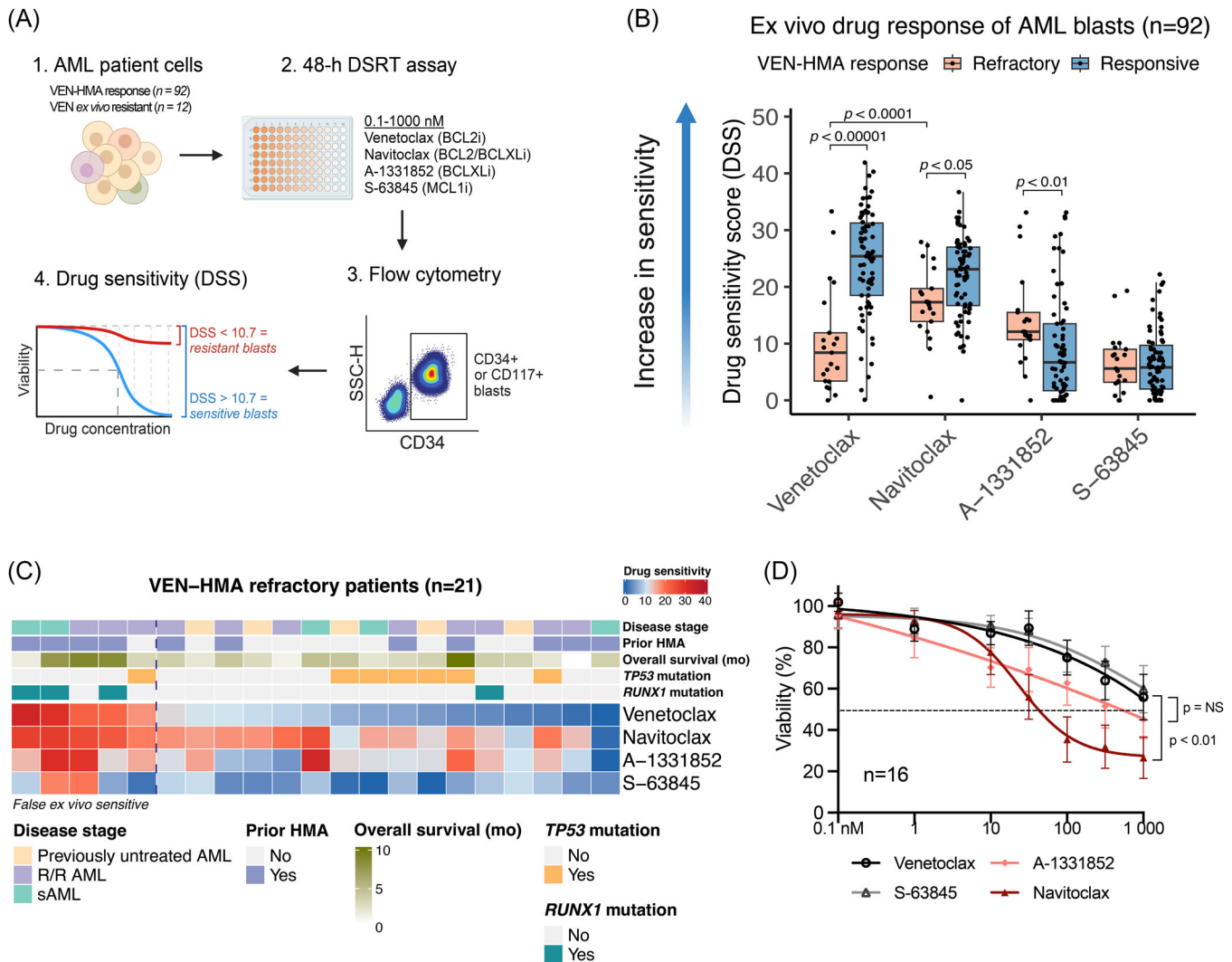


FIGURE 2 Ex vivo drug sensitivity testing with BH3 mimetics identifies susceptibility to BCL-2/BCL-XL inhibition in VEN-HMA-refractory acute myeloid leukemia (AML). (A) Overview of the ex vivo drug sensitivity testing platform. Freshly isolated mononuclear cells from AML patient bone marrow (BM) samples were treated with increasing concentrations of BCL-2 family inhibitors for 48 h. Blast cell (CD34⁺, CD117⁺, or SSC_{low}CD45_{low}) viability was assessed using flow cytometry, and the drug sensitivity score (DSS) was calculated based on the area above the dose-response curve. (B) Ex vivo DSSs to BCL-2 family inhibitors in AML blasts from VEN-HMA refractory ($n = 21$) and responsive ($n = 71$) patients. Wilcoxon rank-sum and paired Wilcoxon signed-rank tests were used to calculate P-values. (C) BCL-2 family drug sensitivity profiles of AML blasts from VEN-HMA refractory patients ($n = 21$). Patients were ordered based on venetoclax DSS. The dashed vertical line highlights samples with false ex vivo VEN sensitivity prediction ($n = 5$). (D) Mean dose-response curves for BCL-2 family inhibitors in blasts from 16 patients with VEN-HMA refractory and ex vivo venetoclax-resistant AML ($DSS < 11.9$). P-values were calculated using an F-test comparing the IC₅₀ values. R/R, relapsed/refractory; sAML, secondary acute myeloid leukemia.

BCL2 expression showed a positive correlation with progenitor-like scores ($R = 0.37$, $P < 0.01$) and a negative correlation with the monocyte-like signature ($R = -0.36$, $P < 0.01$) (Figure 3F). These findings suggest that GMP- and progenitor-like blasts, characterized by favorable BCL-2 family expression, are more likely to be sensitive to venetoclax, while the HSC-like stem cells that rely on alternative anti-apoptotic mechanisms are more common in refractory patients.

VEN-HMA refractory blasts exhibit elevated BCL-XL protein expression relative to BCL-2

To validate the differences in BCL-2 family gene expression at the protein level, we used flow cytometry to quantify the MFI of BCL-2, MCL-1, and BCL-XL in blasts from 47 AML patient samples (clinically

refractory $n = 14$ and responsive $n = 33$). Refractory blasts exhibited significantly higher BCL-XL expression ($P < 0.001$), while BCL-2 was downregulated ($P < 0.01$) (Figure 3G), validating their respective mRNA expression (Supporting Information: Figure S3D). There was no difference in MCL-1 expression, and the observed expression patterns remained consistent in the ND, R/R, and sAML subgroups (Supporting Information: Figure S3E).

We then assessed whether the expression ratio of these anti-apoptotic proteins in blasts could be used to stratify patients according to VEN-HMA response. We calculated two distinct protein expression scores: BCL-XL/BCL-2 and (BCL-XL+MCL-1)/BCL-2. Of these, the BCL-XL/BCL-2 expression ratio ($P < 0.00001$) more effectively distinguished patients by response compared with the score incorporating MCL-1 ($P < 0.01$) (Figure 3H). Collectively, these findings indicate that elevated BCL-XL protein expression

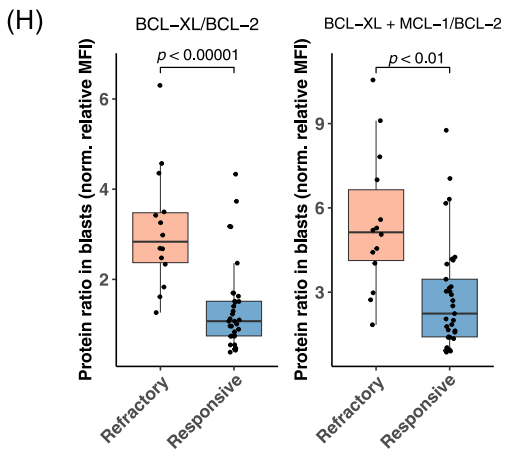
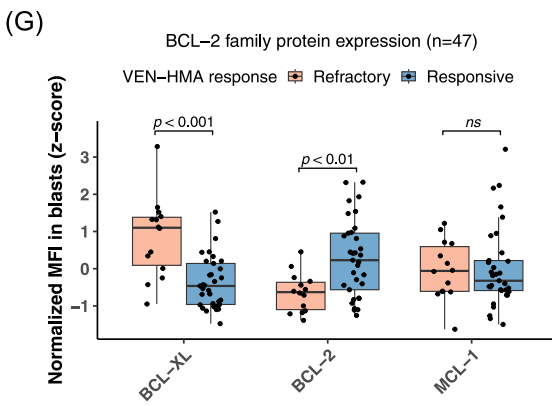
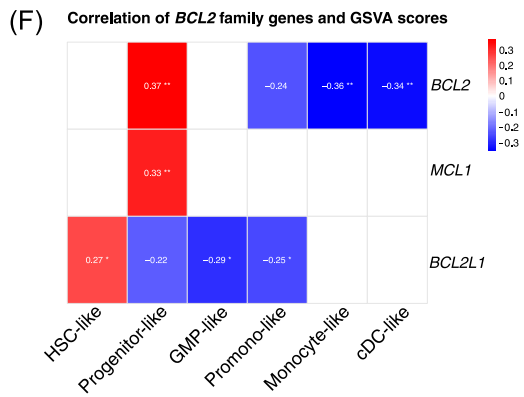
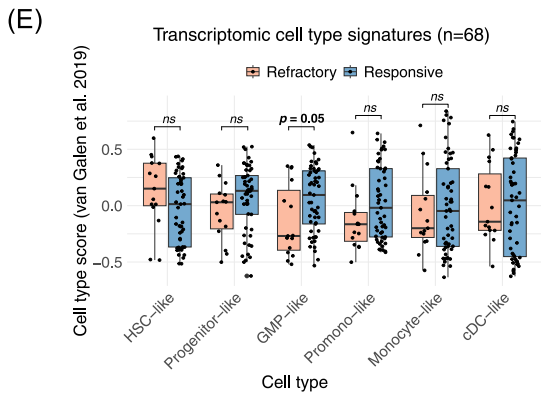
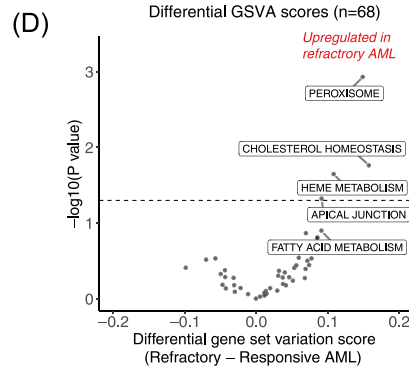
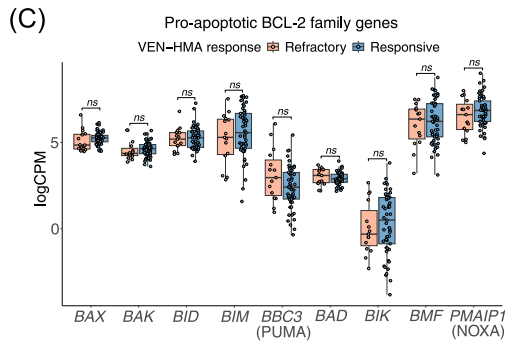
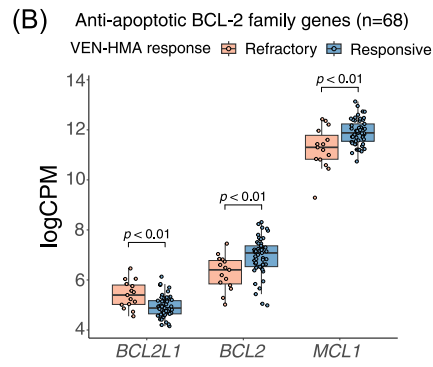
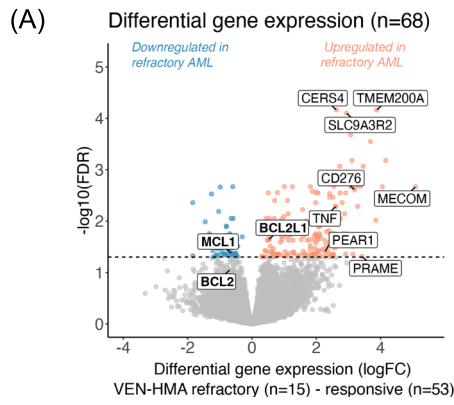


FIGURE 3 Transcriptomic and proteomic data reveal differential anti-apoptotic and phenotypic signatures in VEN-HMA refractory and responsive patients. (A) Differentially expressed genes between blasts enriched from VEN-HMA refractory ($n = 15$) and responsive ($n = 53$) patient samples. Protein-coding genes with counts per million (CPM) ≥ 1 in at least 10% of samples were included. The horizontal line represents the significance threshold at an adjusted P-value of 0.05. (B) Log-transformed CPM expression of anti-apoptotic BCL-2 family genes between VEN-HMA refractory ($n = 15$) and responsive ($n = 53$) patient blasts. (C) Log-transformed CPM expression of pro-apoptotic BCL-2 family genes between VEN-HMA refractory ($n = 15$) and responsive ($n = 53$) patient blasts. (D) Differential Hallmark gene sets identified by gene set variation analysis (GSVA) in blasts from VEN-HMA refractory ($n = 15$) versus responsive ($n = 53$) patients. The t -test was used to calculate P-values. (E) Cell-type signature scores in VEN-HMA refractory ($n = 15$) and responsive ($n = 53$) blasts. Statistical significance was assessed using the Wilcoxon rank-sum test. The center line represents the median. (F) Spearman correlation of 68 samples showing significant correlations ($P < 0.1$) between BCL2 family genes (*BCL2*, *BCL2L1*, and *MCL1*) and myeloid signature GSVA scores. Significant values are annotated with * $P < 0.05$, ** $P < 0.01$. (G) Normalized median fluorescence intensities (MFI) of BCL-XL, BCL-2, and MCL-1 in blasts of VEN-HMA refractory ($n = 14$) and responsive ($n = 33$) patients. Protein MFIs were normalized against a reference sample included in each batch and subsequently converted into z-scores. (H) Protein expression ratios of BCL-XL/BCL-2 and (BCL-XL + MCL-1)/BCL-2 in VEN-HMA refractory and responsive acute myeloid leukemia (AML) blasts. Protein ratios were calculated from normalized relative MFI values, which were obtained by dividing each marker's normalized expression by its cohort median. The Wilcoxon rank-sum test was used in the statistical comparisons unless otherwise specified.

relative to BCL-2 in AML blasts is associated with primary resistance to venetoclax-based therapy.

Genetic and phenotypic predictors of VEN-HMA outcomes

Next, we investigated whether particular genetic or phenotypic subgroups are associated with VEN-HMA outcomes. For phenotypic classification, patients were stratified based on their blast immunophenotype into immature ($CD34^+CD38^-$) or more mature ($CD34^+CD38^+$, $CD34^-CD117^+$, or $CD34^-CD117^-$) groups. Using univariate logistic regression and Cox proportional hazards models, odds ratios for VEN-HMA refractoriness and hazard ratios for survival were estimated in the entire cohort of patients receiving VEN-HMA ($n = 101$) (Figure 4A,B, Supporting Information: Table S10), and then subsequently in the ND ($n = 50$) and R/R/sAML ($n = 51$) patient subgroups (Supporting Information: Figure S4A–D, Supporting Information: Table S11, and Supporting Information: Table S12). In line with prior studies,^{7,11} complex karyotype, *TP53*, and *FLT3-ITD* mutations were associated with refractoriness, while *IDH2* mutations correlated with favorable outcomes (Figure 4A,B). Additionally, the immature blast phenotype ($CD34^+CD38^-$) was associated with refractory response outcomes, consistent with the transcriptomic-level findings on increased LSC17 and HSC-like signatures in refractory blasts (Figure 3E, Supporting Information: Figure S3C).

Because monocytic disease has been linked to venetoclax resistance, we assessed outcomes by the French-American-British (FAB) subtype, which was defined for 69 patients. FAB classification was not associated with treatment response and survival (Supporting Information: Table S10). However, among the 12 patients with myelomonocytic or monocytic AML (FAB M4/M5), only 2 were refractory to VEN-HMA. A similar proportion of refractory patients was observed in FAB M0-2 (12/56) and in patients without a defined FAB subtype (9/32). These results indicate that refractory responses are not restricted to monocytic AML but also occur frequently in immature subtypes.

Differential BCL-2 family dependencies in *IDH2*- and *TP53*-mutated AML

Ex vivo drug sensitivity testing with BCL-2 family inhibitors revealed associations consistent with clinical outcome data: *IDH2*-mutated blasts were the most sensitive to venetoclax (adj. $P = 0.02$), while those harboring *TP53* mutations (adj. $P = 0.04$) and/or complex karyotype (adj. $P = 0.05$) were the most resistant (Figure 4C, Supporting

Information: Table S13). No distinct subgroups with increased sensitivity to A-1331852 or S-63845 were identified, although *TP53*-mutated AML blasts showed a trend toward greater sensitivity to A-1331852 (median DSS *TP53*-mut = 11.5 vs. *TP53*-wt = 6.7) (Supporting Information: Figure S4E).

At the anti-apoptotic BCL-2 family protein level, BCL-XL overexpression was observed in blasts with complex karyotype, all carrying *TP53* mutations ($n = 7$, adj. $P = 0.04$) (Figure 4D, Supporting Information: Table S14). These samples also exhibited the lowest BCL-2 expression in contrast to *IDH2*-mutated blasts with the highest expression (Supporting Information: Table S14). Furthermore, *TP53*-mutated blasts ($n = 9$) had significantly higher BCL-XL/BCL-2 protein expression ratios ($P < 0.01$) compared with *TP53* wild-type samples ($n = 43$) (Figure 4E). Collectively, these findings suggest preferential dependence on BCL-XL in *TP53*-mutated AML and on BCL-2 in *IDH2*-mutated blasts.

TP53-mutated AML exhibits a high protein expression ratio of BCL-XL/BCL2 and sensitivity to SMAC mimetics

Given the poor outcomes in *TP53*-mutated AML, we expanded the original cohort by including samples from 28 *TP53*-mutated patients outside the VenEx study (Supporting Information S1: Supplementary Methods). Importantly, none of these patients received VEN-HMA therapy and therefore were not evaluable for treatment outcome analysis. However, their inclusion enabled a broader investigation of the molecular features of *TP53*-mutated blasts and provided validation for our initial findings. In total, 44 *TP53*-mutated AML samples were profiled, as summarized in Figure 5A.

Multidimensional scaling (MDS) of the transcriptomic profiles of blasts isolated from *TP53*-mutated ($n = 31$) and wild-type patient sample ($n = 65$) revealed distinct clustering based on *TP53* mutation status (Supporting Information: Figure S5A), as well as according to HSC-like gene expression scores, which overlapped with *TP53* status (Supporting Information: Figure S5B). Nearly 5000 differentially expressed genes were identified between *TP53*-mutated and wild-type blasts (adj. P -value < 0.05) (Supporting Information: Table S15). Among these, significant downregulation of *BCL2* and *BAX*, alongside elevated expression of *BCL2L1* (BCL-XL) and *BCL2A1* was observed in *TP53*-mutated blasts (Figure 5B). Pathway enrichment analysis further highlighted strong upregulation of TNF- α /NF- κ B signaling, epithelial-mesenchymal transition (EMT), and IL2-STAT5 signaling in *TP53*-mutated blasts (Figure 5C, Supporting Information: Table S16). As suggested by the MDS analysis (Supporting Information: Figure S5A), *TP53*-mutated blasts showed higher HSC-like gene expression scores ($P < 0.0001$) and reduced progenitor-like scores

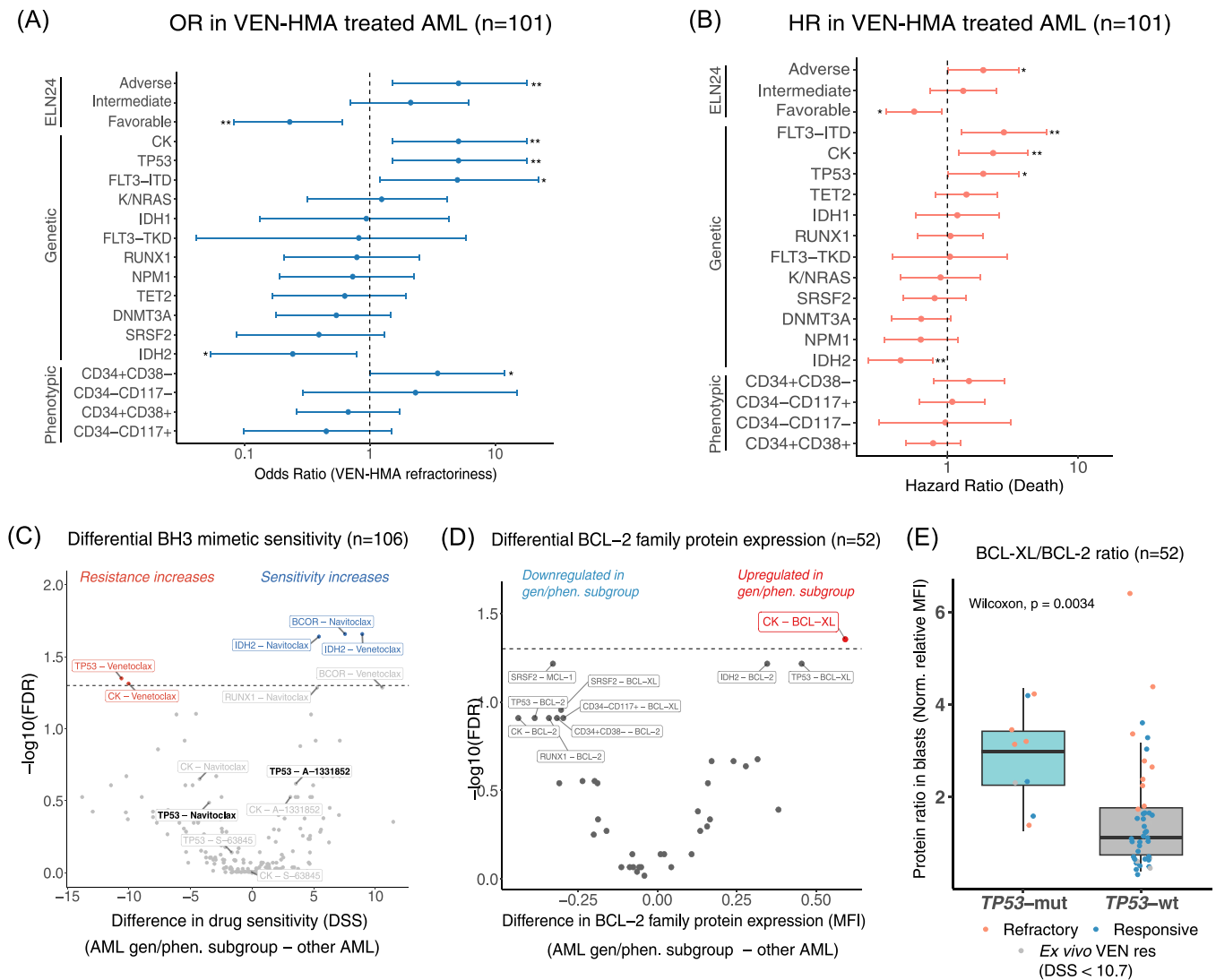


FIGURE 4 Genetic and phenotypic subgroups of acute myeloid leukemia (AML) are associated with VEN-HMA outcomes and ex vivo BH3 mimetic sensitivity. **(A)** Odds ratios (ORs) estimated by univariate logistic regression for refractoriness to VEN-HMA treatment represented as mean OR with corresponding 95% confidence intervals (CIs). ELN24 risk categories: adverse = *TP53*-mut, intermediate = *FLT3*-ITD or *NRAS*/*KRAS*-mut, favorable = all other cases. Blast phenotypes: $CD34^+CD38^-$ (>40% blasts), $CD34^+CD38^+$ (>60% blasts), $CD34^-CD117^+$ (>90% blasts), and $CD34^-CD117^-$ (>95% blasts). * $P < 0.05$, ** $P < 0.01$. **(B)** Hazard ratios (HRs) for death analyzed by Cox proportional hazards regression represented as mean HR with lower and upper CI bounds. * $P < 0.05$, ** $P < 0.01$. **(C)** Differential ex vivo sensitivities to BH3 mimetics between genotypic or phenotypic AML subgroups compared to wild-type counterparts. The analysis included ex vivo venetoclax-resistant patients ($n = 12$) and two patients with non-evaluable response. Each dot represents the mean difference in drug sensitivity scores. Statistical significance was determined using the Wilcoxon rank-sum test, with P-values adjusted using the FDR method. **(D)** Differential BCL-2 family protein expression between AML subgroups with specific genetic alterations or phenotypic features compared to their wild-type counterparts. The analysis included ex vivo venetoclax-resistant patients ($n = 5$). Statistical difference was calculated using the Wilcoxon rank-sum test, with P-values adjusted using the FDR method. **(E)** BCL-XL/BCL-2 protein expression ratios in *TP53*-mutated ($n = 9$) and wild-type ($n = 43$) AML blasts. Normalized median fluorescence intensities of BCL-XL and BCL-2 measured by flow cytometry were divided by the cohort median of each marker to gain relative values, which were then used to derive BCL-XL/BCL-2 ratios. The Wilcoxon rank-sum test was used to calculate P-values. FDR, false discovery rate; MFI, median fluorescence intensity.

($P < 0.0001$) (Supporting Information: Figure S5C), reflecting the transcriptional profile of VEN-HMA refractory blasts (Figure 3E).

Flow cytometry analysis confirmed elevated BCL-XL/BCL-2 protein expression ratios in *TP53*-mutated blasts ($P < 0.05$, *TP53*-mut $n = 31$, *TP53*-wt $n = 43$) (Figure 5D). Consistent with this, 48 h ex vivo treatment with venetoclax induced significantly less cell death in *TP53*-mutated blasts ($n = 35$) compared to wild type ($n = 90$, $P < 0.0001$) (Figure 5E). However, the BCL-XL inhibitor A-1331852 efficacy was generally modest among *TP53*-mutated AML (Figure 5E), although seven ex vivo venetoclax-resistant

samples showed marked sensitivity to BCL-XL and/or BCL-2/BCL-XL inhibitors (Supporting Information: Figure S5D).

To further explore potential therapeutic vulnerabilities in this high-risk subgroup, we analyzed drug sensitivity data from an independent AML cohort comprising 78 samples, including 11 with *TP53* mutations and/or del(17). Among 37 tested compounds, the SMAC mimetic LCL-161 was the only drug showing enhanced activity in *TP53*-mutated blasts (Figure 5F, Supporting Information: Figure S5E). However, in our extended *TP53*-mutated cohort, SMAC mimetic sensitivity did not differ significantly from wild type ($P = 0.06$, Supporting Information:

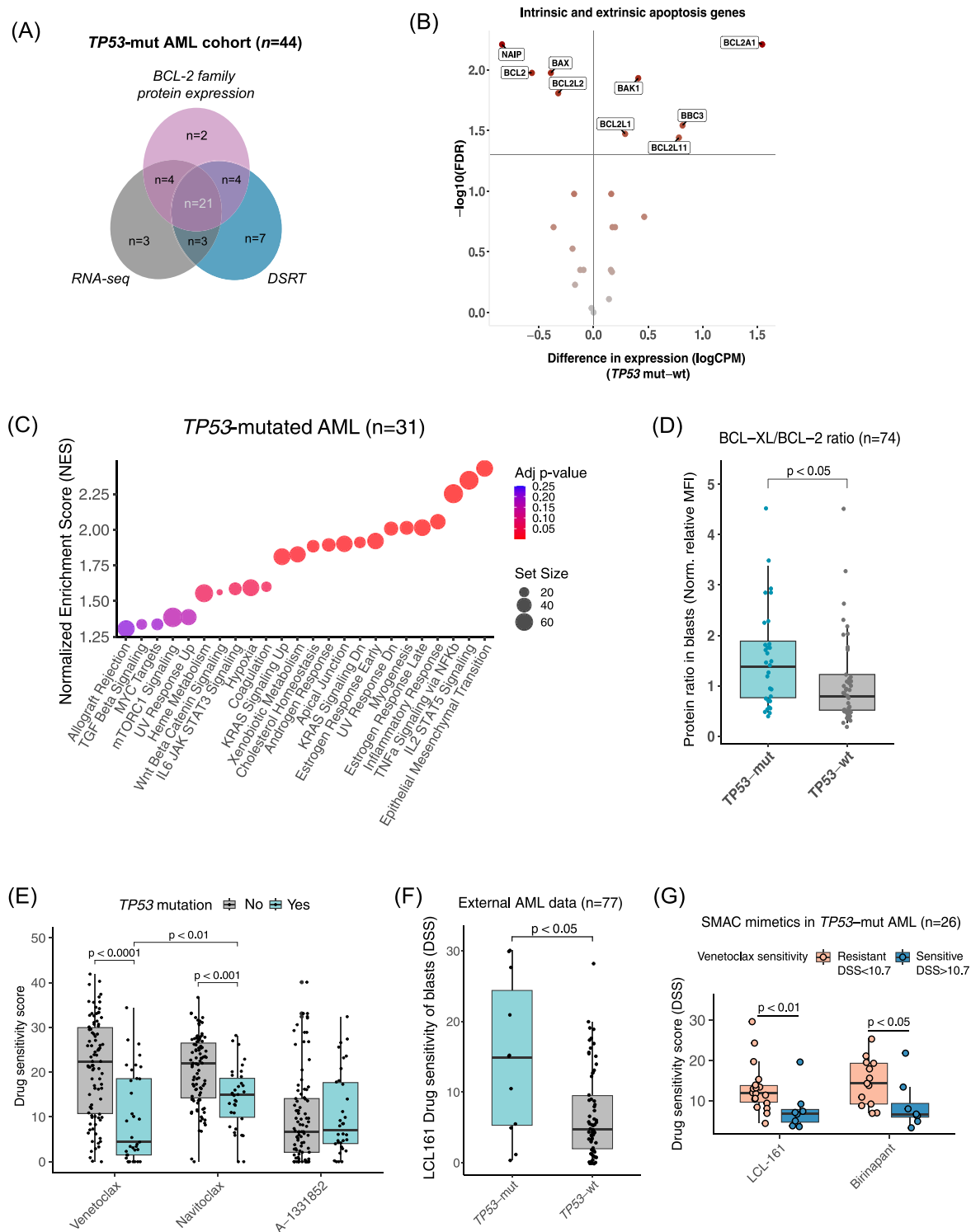


FIGURE 5 *TP53*-mutated acute myeloid leukemia (AML) blasts share similar molecular features with VEN-HMA refractory AML. (A) Venn diagram depicting the overlap of molecular and functional data in the *TP53*-mutated AML cohort. In total, 28 samples were obtained outside the VenEx trial, consisting of newly diagnosed ($n = 24$), relapsed/refractory (R/R) ($n = 1$), and secondary AML ($n = 3$) patients. (B) Differential expression of selected intrinsic and extrinsic apoptosis pathway genes between *TP53*-mutated ($n = 31$) and *TP53* wild-type ($n = 65$) AML blasts. Student's t -test was used to compare the mean log counts per million (CPM), and P-values were adjusted with FDR. (C) Upregulated Hallmark gene sets in *TP53*-mutated AML samples ($n = 31$) identified by GSEA. (D) BCL-XL/BCL-2 protein ratios in *TP53*-mutated ($n = 31$) and *TP53* wild-type ($n = 43$) AML blasts. Median fluorescence intensities of BCL-XL and BCL-2, measured by flow cytometry and normalized to a reference sample, were converted to relative values by dividing each marker by the cohort median. These normalized values were subsequently converted to BCL-XL/BCL-2 ratios. (E) Ex vivo sensitivity scores for venetoclax, navitoclax, and A-1331852 obtained via flow cytometry from blasts of *TP53*-mutated ($n = 35$) and *TP53* wild-type ($n = 90$) AML patients. (F) Ex vivo LCL-161 drug sensitivity scores (DSS) of AML blasts with *TP53* mutations and/or del(17) ($n = 11$) versus *TP53* wild type ($n = 66$). This drug sensitivity dataset was obtained outside the study. (G) Ex vivo sensitivity of blasts to LCL-161 and birinapant from *TP53*-mutated AML patient samples stratified based on their ex vivo venetoclax response (resistant AML = DSS < 10.7 $n = 17$, sensitive AML = DSS > 10.7 $n = 9$). Statistical comparisons were done using the Wilcoxon rank-sum test unless otherwise specified. FDR, false discovery rate; GSEA, gene set enrichment analysis.

Figure S5F), but increased SMAC mimetic efficacy was observed in *TP53*-mutated samples exhibiting *ex vivo* venetoclax resistance (DSS < 10.7) (Figure 5G).

Together, these findings suggest that *TP53*-mutated AML shares molecular features with VEN-HMA refractory blasts, including increased BCL-XL/BCL2 protein expression ratio and HSC-like transcriptomic signatures, which might contribute to venetoclax resistance.

VEN-HMA refractory AML blasts upregulate TNF and display increased sensitivity to SMAC mimetics

Given the observed SMAC mimetic sensitivity in *ex vivo* venetoclax-resistant *TP53*-mutated blasts, we next evaluated their therapeutic potential in VEN-HMA refractory blasts. Sensitivity to SMAC mimetics has previously been associated with enhanced TNF signaling,^{47,48} and we detected upregulated TNF expression in refractory blasts (Figures 3A and 6A).

Since TNF is predominantly expressed in monocytes, we first analyzed TNF expression across AML differentiation stages based on FAB classification. As hypothesized, blasts enriched from monocytic FAB M5 samples exhibited the highest TNF expression (Supporting Information: Figure S6A). However, elevated TNF expression was linked to VEN-HMA refractoriness, particularly in FAB M0-M2 subtypes, but not in FAB M4-M5 (monocytic) samples (Figure 6B). Importantly, blasts from refractory patients displayed increased sensitivity to the SMAC mimetics LCL-161 and birinapant in a 48 h *ex vivo* assay ($P < 0.05$) (Figure 6C). Furthermore, SMAC mimetic sensitivity correlated with elevated TNF expression in blasts, including those analyzed in the external *TP53*-mutated AML cohort ($R = 0.44$, $P < 0.001$) (Figure 6D).

To investigate whether secreted TNF is associated with resistance, we measured soluble TNF protein concentration along with 44 other inflammatory cytokines from the BM-derived plasma of 89 patients (Target 48, Olink, Supporting Information: Table S17). However, TNF levels were not higher in VEN-HMA refractory patients compared to responsive patients (Supporting Information: Figure S6B). Within the full cytokine panel, chemokine ligand CCL19, blood vessel formation regulator vascular endothelial growth factor A (VEGF-A), and macrophage colony-stimulating factor CSF1 showed increased concentrations in the BM plasma of refractory patients (Supporting Information: Figure S6C).

Because TNF acts upstream of SMAC mimetic targets cIAP1/2 and XIAP, we examined whether TNF exposure modulates drug response. Simultaneous treatment with soluble TNF (10 ng/mL) and birinapant or venetoclax did not enhance SMAC mimetic sensitivity or induce venetoclax resistance, respectively (Supporting Information: Figure S6D). Similarly, the TNF-blocking antibody infliximab had no impact on drug sensitivity. Together, these findings suggest that SMAC mimetic sensitivity in refractory blasts is likely driven by molecular mechanisms beyond TNF stimulation alone.

Combinations of BCL-2 family inhibitors and SMAC mimetics overcome venetoclax resistance but impact healthy HSPCs

Next, we explored whether BCL-2 family inhibitors (venetoclax, navitoclax, or A-1331852) in combination with SMAC mimetics (LCL-161 or birinapant) could enhance the efficacy of targeting of VEN-HMA refractory blasts. Using 48 h *ex vivo* drug testing, we analyzed three VEN-HMA refractory and five *ex vivo* venetoclax-resistant samples (DSS < 10.7). All the six drug combinations outperformed their respective single-drug treatments, with the highest efficacy obtained with the combination of navitoclax + LCL-161, reducing blast viability by

>70% compared to 25% with venetoclax alone (Figure 6E). Further synergy analysis using 8 × 8 drug matrices revealed synergy between all the tested combinations, with the strongest synergy observed for A-1331852 + SMAC mimetics drug combinations (Figure 6F, Supporting Information: Table S18).

To assess potential toxicity, we tested BH3 and SMAC mimetic combinations on CD34⁺ hematopoietic stem and progenitor cells (HSPCs) from two healthy donors. In a colony-forming assay, both navitoclax + LCL-161 and A-1331852 + LCL-161 combinations markedly suppressed erythroid colony formation (BFU/CFU-E), while granulocyte/macrophage colonies (CFU-GM) were partially spared (Figure 6G). Similar cytotoxicity was observed in a 48-h *ex vivo* drug combination screen, where both combinations reduced healthy CD34⁺ HSPCs to the same extent as refractory blasts (Supporting Information: Figure S6E). Together, these findings indicate that while dual targeting of BCL-XL/BCL-2 and IAPs can effectively eradicate venetoclax-resistant blasts, it also carries toxicity to healthy HSCs.

DISCUSSION

While venetoclax has improved outcomes in AML, a significant number of patients exhibit upfront resistance. In this study, we profiled blasts from AML patients prior to VEN-HMA treatment to identify molecular signatures of primary resistance and explored alternative therapeutic strategies. Blasts from refractory patients were characterized by an elevated protein expression ratio of BCL-XL/BCL-2, an immature CD34⁺CD38⁻ blast phenotype, and frequent *TP53* mutations. Functionally, refractory blasts displayed sensitivity to dual BCL-XL/BCL-2 inhibition and SMAC mimetics.

AML BM contains non-blast cell populations that can mask the molecular features of leukemic blasts. We therefore restricted our analysis to CD34⁺ blasts, and in cases lacking CD34 expression, to CD117⁺ blasts. These are well-established markers of immature myeloid blasts and are considered to capture cell populations containing LSCs.^{49,50} In these blasts, elevated BCL-XL relative to BCL-2 emerged as a key feature of clinical resistance, consistent with previous studies by Waclawiczek et al. and Knopleva et al.^{13,32} Accordingly, refractory blasts exhibited higher sensitivity to the dual BCL-2/BCL-XL inhibitor navitoclax than venetoclax, whereas sensitivity to selective BCL-XL inhibition was limited to a subset of patients.

Monocytic AML has been associated with VEN-HMA resistance, consistent with the increased MCL-1 expression in this lineage.^{19,23,51,52} A recent large study reported inferior survival outcomes in monocytic AML, except in patients with *NPM1* mutations.³⁰ Also, erythroid differentiation has been linked to resistance through BCL-XL upregulation.^{24,53} In our cohort ($n = 101$), among 23 refractory patients, two had monocytic AML (FAB M4-5), 12 had FAB M0-M2 morphology, and nine had undefined FAB subtype, indicating that resistance is also common in immature subtypes and that the majority of refractory cases in our study originated from non-monocytic AML. In contrast to prior reports, we did not observe increased MCL-1 expression or sensitivity to MCL1 inhibition in refractory blasts, possibly resulting from the low number of monocytic cases. Thus, the resistance features identified here may not represent those driving resistance in monocytic AML.

Even among the studied blast populations, we observed phenotypic heterogeneity, with the immature CD34⁺CD38⁻ phenotype enriched in refractory patients, consistent with findings by Stahl et al.²⁵ Transcriptomic analyses supported this observation, showing elevated LSC17 scores and a trend toward a higher HSC-like signature in blasts from refractory patients, whereas GMP-like

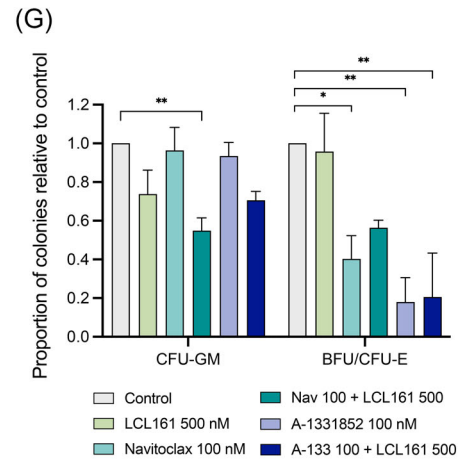
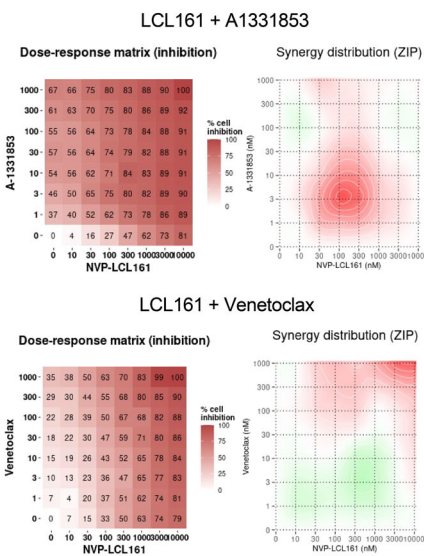
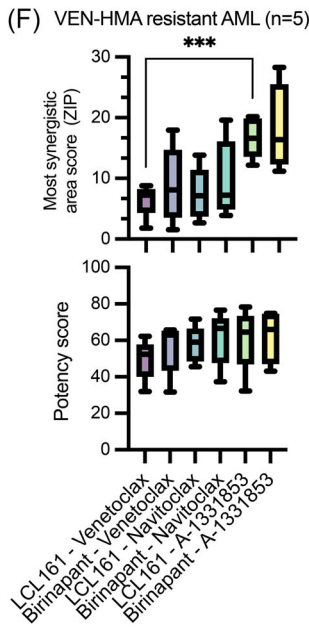
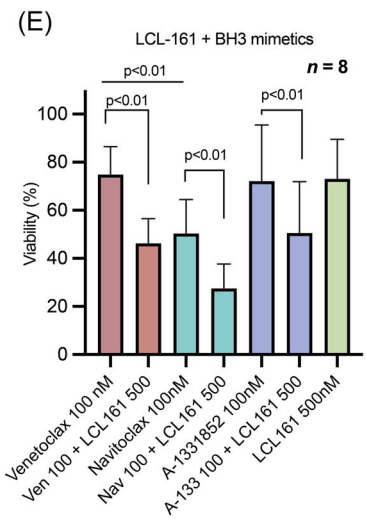
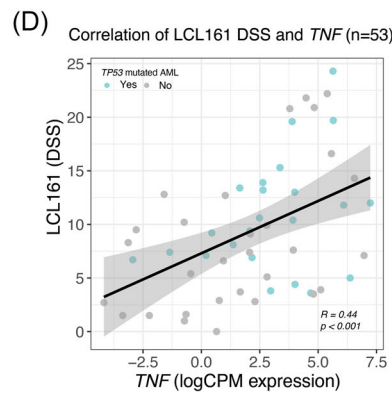
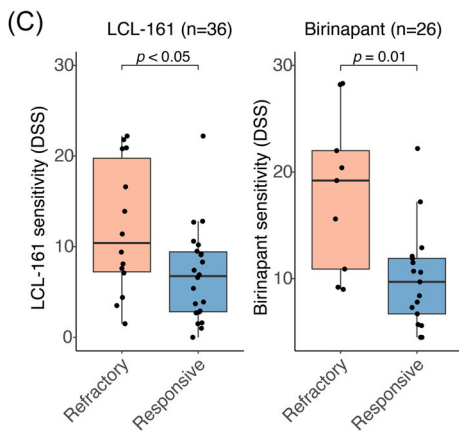
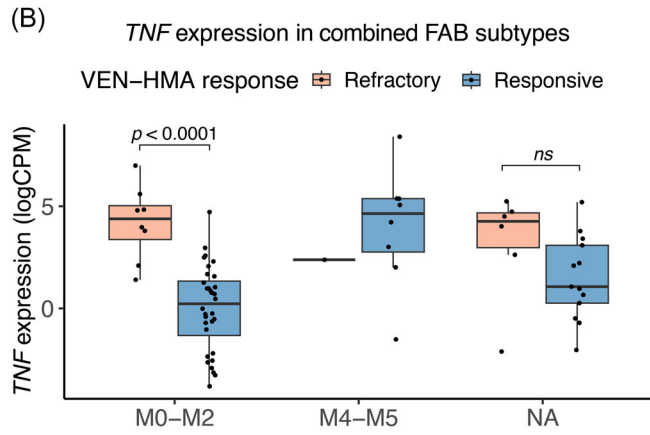
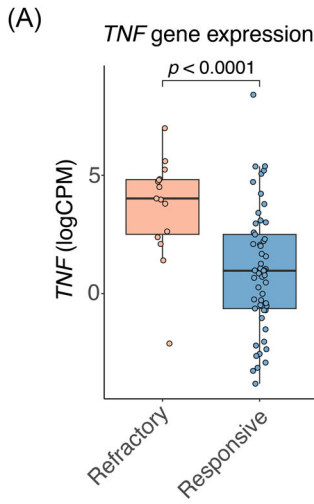


FIGURE 6 Blasts from venetoclax (VEN)–hypomethylating agent (HMA) refractory AML patients overexpress *TNF*, which correlates with sensitivity to SMAC mimetics. (A) *TNF* gene expression as log-transformed counts per million (CPM) in AML blasts enriched from VEN–HMA refractory ($n = 15$) and responsive patient samples ($n = 53$). (B) *TNF* log-transformed CPM gene expression across the combined French–American–British (FAB) AML subtypes (M0–M2 $n = 43$, M4–M5 $n = 9$, and NA $n = 22$) with grouping based on response to VEN–HMA therapy. (C) Ex vivo sensitivity of blasts to the SMAC mimetics LCL-161 ($n = 36$) and birinapant ($n = 26$) from AML patients stratified based on VEN–HMA response. (D) Spearman correlation of LCL-161 drug sensitivity score (DSS) and *TNF* expression in blasts of AML samples ($n = 53$). (E) Viability of blasts from VEN–HMA refractory ($n = 3$) or ex vivo VEN-resistant ($n = 5$) patients after 48 h treatment with single drugs (venetoclax, navitoclax, A-1331852, and LCL-161) or the combinations of BCL-2 inhibitors and LCL-161 with selected concentrations. (F) Most synergistic area (2×2 area) and potency scores of BH3 (venetoclax, navitoclax, or A-1331852) and SMAC mimetic (LCL-161 or birinapant) combinations. Bulk mononuclear cells (MNCs) from three VEN–HMA refractory and two ex vivo VEN-resistant samples were assessed using a 48 h CellTiter-Glo viability assay (left). Representative synergy matrices for LCL-161 + A-1331852 and LCL-161 + venetoclax combinations in one resistant index patient (right). (G) Relative colony-forming unit-granulocyte/macrophage (CFU-GM) and burst-forming unit/Colony-forming unit-erythroid (BFU/CFU-E) colony counts on Day 14 from bone marrow (BM) mononuclear cells of two healthy donors treated with the SMAC mimetic LCL161 and the BH3 mimetics A-1331852 and navitoclax alone or in combination. Cells were pre-treated for 24 h with the indicated concentrations and subsequently plated in semi-solid medium containing the same treatments. Results represent median \pm SD of two donors tested in duplicate. * $P < 0.05$, ** $P < 0.01$.

signatures correlated with VEN–HMA sensitivity. Contrary to the commonly held view of immature blasts being sensitive to BCL-2 inhibition,^{54,55} our results suggest additional complexity in blast/LSC biology. Specifically, HSC-like stem cells appear to be associated with VEN–HMA resistance, while more differentiated progenitor-like blasts remain sensitive. However, the contributions of cell type versus mutational background remain unresolved; for example, *TP53*-mutated patients often show an HSC-signature, whereas *IDH2*/*NPM1*-mutations align with GMP-like states.⁵⁶

TP53 mutations are the strongest genetic predictor of poor outcomes with VEN–HMA therapy,¹¹ as was also seen in our cohort. To further investigate the molecular characteristics of this AML subtype, we expanded our cohort to include a total of 44 patients with *TP53* mutation. Like VEN–HMA refractory blasts, *TP53*-mutated blasts exhibited an elevated ratio of BCL-XL/BCL-2 protein expression and immature HSC-like gene expression. In addition, reduced *BAX* expression and heightened inflammatory signaling (*TNF- α* /*NF- κ B* and *IL-2*-STAT5) were identified in *TP53*-mutated AML. These features may contribute to poor venetoclax responses consistently observed in *TP53*-mutated AML.

TNF was one of the most upregulated genes in VEN–HMA refractory blasts. Since elevated *TNF* expression has been linked with SMAC mimetic sensitivity in AML,^{48,57} we hypothesized that activating the extrinsic apoptotic pathway with SMAC mimetics could be effective. *TNF* can drive both cell survival and death, the latter being blocked by cIAPs. SMAC mimetics antagonize cIAP1/2 and XIAP, restoring cell death signaling. We found that SMAC mimetics were effective against VEN–HMA refractory blasts, with *TNF* expression correlating with drug response. Earlier reports have also demonstrated SMAC mimetic activity in VEN-resistant AML models.⁵⁸ However, neither soluble *TNF* stimulation nor *TNF* blockade with infliximab altered sensitivity to SMAC mimetics or venetoclax. Furthermore, *TNF* levels in BM plasma did not differ between refractory and responsive patients. Together, these results suggest that sensitivity to SMAC mimetics is driven by intrinsic cellular factors rather than *TNF* stimulation alone. Further studies are required to elucidate the mechanisms behind this association, potentially leading to the identification of novel therapeutic targets.

Despite promising preclinical data, SMAC mimetics have shown limited efficacy as monotherapies in clinical trials.^{59,60} However, in myelofibrosis, a disease characterized by a *TNF*-rich microenvironment, LCL-161 monotherapy has demonstrated clinical activity.⁶¹ In our assays, SMAC mimetics combined with BCL-XL/BCL-2 inhibitors eliminated venetoclax-resistant blasts. However, this combination also induced toxicity in healthy CD34⁺ HSCs. Moreover, the BCL-XL/BCL-2 inhibitor navitoclax has faced clinical challenges due to thrombocytopenia,^{62,63} and while selective BCL-XL inhibitors have been tolerable in rodents, they have revealed cardiovascular

toxicities in higher primates.⁶⁴ These limitations pose challenges for direct clinical translation. Nevertheless, emerging approaches such as antibody–drug conjugates (ADCs) and PROTACs may allow for more selective targeting of leukemic cells while mitigating toxicities.^{64–67}

We acknowledge several limitations of this study. First, the patient cohort was heterogeneous, including ND, R/R, and sAML patients, which may have distinct resistance mechanisms; importantly, most refractory cases in our cohort occurred within the R/R/sAML. Second, although blast enrichment improved the specificity of molecular profiling, it may not capture the relevant and comparable blast populations in all subtypes, such as in monocytic AML, where CD33-based enrichment was applied in two cases. The use of more refined stem cell markers or single-cell profiling approaches could provide greater resolution. Finally, the lack of in vivo validation of candidate drugs limits the translational potential of our findings.

In conclusion, our study provides new insight into the mechanisms underlying VEN–HMA resistance in AML. These findings highlight potential therapeutic vulnerabilities and point to opportunities for developing more effective treatment strategies for venetoclax refractory disease.

ACKNOWLEDGMENTS

We thank the patients, their families, physicians, and study nurses for their participation in the study. We also acknowledge the expert technical support provided by the FIMM High Throughput Biomedicine Unit and the FIMM Genomics NGS Sequencing Unit, both hosted by the University of Helsinki and supported by HiLIFE and Biocenter Finland. We are grateful to Professor Kimmo Porkka for providing the eCare4me AML patient drug sensitivity data used for exploring therapeutic vulnerabilities in *TP53*-mutated AML. We further thank the members of Professor Andreas Trumpp's laboratory, especially Alexander Waclawiczek, Aino-Maija Leppä and Simon Renders for sharing the protocol for flow cytometry-based quantification of BCL-2 family protein expression. With deep appreciation, we remember Professor Ilya Shmulevich, whose invaluable insights and generous spirit continue to inspire our work. Graphical illustrations were created using a BioRender.com license, and ChatGPT was utilized for proofreading assistance. Open access publishing facilitated by Helsingin yliopisto, as part of the Wiley - FinELib agreement.

AUTHOR CONTRIBUTIONS

Ida Vääntinen: Conceptualization; data curation; formal analysis; funding acquisition; methodology; investigation; project administration; visualization; writing—original draft; writing—review and editing.
Joseph Saad: Conceptualization; methodology; data curation;

investigation; formal analysis; visualization; project administration; writing—original draft; writing—review and editing. **Tanja Ruokoranta:** Investigation; methodology; writing—review and editing. **Sari Kytölä:** Data curation; resources; writing—review and editing. **Guangrong Qin:** Formal analysis; investigation; funding acquisition; writing—review and editing. **Bahar Tercan:** Investigation; formal analysis; funding acquisition; writing—review and editing. **Pia Ettala:** Writing—review and editing; resources. **Anu Partanen:** Resources; writing—review and editing. **Marja Pyörälä:** Resources; writing—review and editing. **Johanna Rimpiläinen:** Resources; writing—review and editing. **Timo Siitonen:** Resources; writing—review and editing. **Mikko Manninen:** Resources. **Peter J. M. Valk:** Resources; writing—review and editing. **Gerwin Huls:** Resources. **Vésteinn Thorsson:** Funding acquisition; writing—review and editing. **Caroline A. Heckman:** Funding acquisition. **Mika Kontro:** Conceptualization; data curation; funding acquisition; investigation; project administration; resources; supervision; writing—review and editing. **Heikki Kuusanmäki:** Conceptualization; data curation; formal analysis; funding acquisition; investigation; methodology; project administration; resources; supervision; visualization; writing—original draft; writing—review and editing.

CONFLICT OF INTEREST STATEMENT

A.P. reports personal fees from AbbVie, AstraZeneca, Behring, Janssen-Cilag, Novartis, Sanofi, and Takeda. C.A.H. reports research funding from Novartis, Orion Pharma, Bristol Myers Squibb/Celgene, Oncopeptides, and Kronos Bio Inc., and personal fees from Oncopeptides. P.E. reports personal fees from Novartis, Pfizer, Amgen, and Sanofi. M.P. reports personal fees from Pfizer, Novartis, and AbbVie. J.R. reports personal fees from Astellas Pharma, AbbVie, Bristol Myers Squibb, and Pfizer. T.S. reports personal fees from Bristol Myers Squibb, Amgen, GSK, Janssen-Cilag, AbbVie, and Otsuka Pharma. H.K. reports research funding from AbbVie (outside the submitted work) and personal fees from Faron. M.K. reports personal fees from Astellas Pharma, AbbVie, Bristol Myers Squibb, Faron Pharmaceuticals, Novartis, and Pfizer, and research funding from AbbVie (outside the submitted work). The remaining authors declare no competing financial interests.

DATA AVAILABILITY STATEMENT

Clinical, molecular, and drug sensitivity data are available in the supplementary files. RNA-sequencing data generated in this study have been deposited in the Zenodo database under doi:10.5281/zenodo.17777357.

FUNDING

This study was supported by the Cancer Foundation Finland, the Finnish Medical Foundation, the Helsinki University Hospital Comprehensive Cancer Center, the University of Helsinki, the iCAN-Digital Precision Medicine Flagship, the Sigrid Juselius Foundation and the National Cancer Institute of the National Institutes of Health under award number R01CA270210. H.K. is supported by the Finnish Cultural Foundation, H.K. and I.V. are supported by the Orion Research Foundation, and H.K. and M.K. are supported by the Foundation for the Finnish Cancer Institute. Open access publishing facilitated by Helsingin yliopisto, as part of the Wiley - FinELib agreement.

SUPPORTING INFORMATION

Additional supporting information can be found in the online version of this article.

ORCID

Ida Vänttinen  <https://orcid.org/0009-0002-9764-3477>

Joseph Saad  <https://orcid.org/0000-0001-7701-0328>

Caroline A. Heckman  <https://orcid.org/0000-0002-4324-8706>

REFERENCES

- DiNardo CD, Erba HP, Freeman SD, Wei AH. Acute myeloid leukaemia. *Lancet*. 2023;401:2073-2086.
- DiNardo CD, Jonas BA, Pullarkat V, et al. Azacitidine and venetoclax in previously untreated acute myeloid leukemia. *N Engl J Med*. 2020;383:617-629.
- DiNardo CD, Pratz K, Pullarkat V, et al. Venetoclax combined with decitabine or azacitidine in treatment-naive, elderly patients with acute myeloid leukemia. *Blood*. 2019;133:7-17.
- Angotzi F, Lessi F, Leoncin M, et al. Efficacy and safety of venetoclax plus hypomethylating agents in relapsed/refractory acute myeloid leukemia: a multicenter real-life experience. *Front Oncol*. 2024;14:1370405.
- DiNardo CD, Rausch CR, Benton C, et al. Clinical experience with the BCL2-inhibitor venetoclax in combination therapy for relapsed and refractory acute myeloid leukemia and related myeloid malignancies. *Am J Hematol*. 2018;93:401-407.
- Tenold ME, Moskoff BN, Benjamin DJ, et al. Outcomes of adults with relapsed/refractory acute myeloid leukemia treated with venetoclax plus hypomethylating agents at a comprehensive cancer center. *Front Oncol*. 2021;11:11.
- DiNardo CD, Tiong IS, Quagliari A, et al. Molecular patterns of response and treatment failure after frontline venetoclax combinations in older patients with AML. *Blood*. 2020;135:791-803.
- Gangat N, Elbeih A, Ghosoun N, et al. Mayo genetic risk models for newly diagnosed acute myeloid leukemia treated with venetoclax + hypomethylating agent. *Am J Hematol*. 2025;100:260-271.
- Lachowiec CA, Ravikumar VI, Othman J, et al. Refined ELN 2024 risk stratification improves survival prognostication following venetoclax-based therapy in AML. *Blood*. 2024;144:2788-2792.
- Bataller A, Bazinet A, DiNardo CD, et al. Prognostic risk signature in patients with acute myeloid leukemia treated with hypomethylating agents and venetoclax. *Blood Adv*. 2024;8:927-935.
- Döhner H, Pratz KW, DiNardo CD, et al. Genetic risk stratification and outcomes among treatment-naive patients with AML treated with venetoclax and azacitidine. *Blood*. 2024;144:2211-2222.
- Döhner H, DiNardo CD, Appelbaum FR, et al. Genetic risk classification for adults with AML receiving less-intensive therapies: the 2024 ELN recommendations. *Blood*. 2024;144:2169-2173.
- Waclawiczek A, Leppä AM, Renders S, et al. Combinatorial BCL2 family expression in acute myeloid leukemia stem cells predicts clinical response to azacitidine/venetoclax. *Cancer Discov*. 2023;13:1408-1427.
- Ramsey HE, Fischer MA, Lee T, et al. A novel MCL1 inhibitor combined with venetoclax rescues venetoclax-resistant acute myelogenous Leukemia. *Cancer Discov*. 2018;8:1566-1581.
- Fischer MA, Song Y, Arrate MP, et al. Selective inhibition of MCL1 overcomes venetoclax resistance in a murine model of myelodysplastic syndromes. *Haematologica*. 2023;108:522-531.
- Stevens BM, Jones CL, Pollyea DA, et al. Fatty acid metabolism underlies venetoclax resistance in acute myeloid leukemia stem cells. *Nat Cancer*. 2020;1:1176-1187.
- Wang B, Reville PK, Yassouf MY, et al. Comprehensive characterization of IFN γ signaling in acute myeloid leukemia reveals prognostic and therapeutic strategies. *Nat Commun*. 2024;15:1821.
- Karjalainen R, Pemovska T, Popa M, et al. JAK1/2 and BCL2 inhibitors synergize to counteract bone marrow stromal cell-induced protection of AML. *Blood*. 2017;130:789-802.
- Kuusanmäki H, Leppä AM, Pölonen P, et al. Phenotype-based drug screening reveals association between venetoclax response and

- differentiation stage in acute myeloid leukemia. *Haematologica*. 2020;105:708-720.
20. White BS, Khan SA, Mason MJ, et al. Bayesian multi-source regression and monocyte-associated gene expression predict BCL-2 inhibitor resistance in acute myeloid leukemia. *npj Precis Oncol*. 2021;5:71.
 21. Bottomly D, Long N, Schultz AR, et al. Integrative analysis of drug response and clinical outcome in acute myeloid leukemia. *Cancer Cell*. 2022;40:850-864.e9.
 22. Zhang H, Nakauchi Y, Köhnke T, et al. Integrated analysis of patient samples identifies biomarkers for venetoclax efficacy and combination strategies in acute myeloid leukemia. *Nat Cancer*. 2020;1:826-839.
 23. Pei S, Pollyea DA, Gustafson A, et al. Monocytic subclones confer resistance to venetoclax-based therapy in patients with acute myeloid leukemia. *Cancer Discov*. 2020;10:536-551.
 24. Kuusanmäki H, Dufva O, Vähä-Koskela M, et al. Erythroid/megakaryocytic differentiation confers BCL-XL dependency and venetoclax resistance in acute myeloid leukemia. *Blood*. 2023;141:1610-1625.
 25. Stahl M, Menghrajani K, Derkach A, et al. Clinical and molecular predictors of response and survival following venetoclax therapy in relapsed/refractory AML. *Blood Adv*. 2021;5:1552-1564.
 26. Maiti A, Konoplev S, DiNardo CD, et al. Outcomes of de novo acute myeloid leukemia with monocytic differentiation (FAB M4/5) treated with venetoclax and decitabine. *Blood*. 2020;136:11-13.
 27. Zhao L, Yang J, Chen M, et al. Myelomonocytic and monocytic acute myeloid leukemia demonstrate comparable poor outcomes with venetoclax-based treatment: a monocentric real-world study. *Ann Hematol*. 2024;103:1197-1209.
 28. Jin D, He J, Chen H, et al. Impact of monocytic differentiation on acute myeloid leukemia patients treated with venetoclax and hypomethylating agents. *Cancer Med*. 2024;13:e7378.
 29. Zhao LP, Dumas-Rivero T, Barette L, et al. Prognostic significance of monocytic-like phenotype in patients with AML treated with venetoclax and azacytidine. *Blood Adv*. 2025;9(14):3556-3565.
 30. Lachowicz CA, Heiblig M, Aspas Requena G, et al. Genetic and phenotypic correlates of clinical outcomes with venetoclax in acute myeloid leukemia: the GEN-PHEN-VEN study. *Blood Cancer Discov*. 2025;6(5):437-449.
 31. Wegmann R, Bonilla X, Casanova R, et al. Single-cell landscape of innate and acquired drug resistance in acute myeloid leukemia. *Nat Commun*. 2024;15:9402.
 32. Konopleva M, Pollyea DA, Potluri J, et al. Efficacy and biological correlates of response in a phase II study of venetoclax monotherapy in patients with acute myelogenous leukemia. *Cancer Discov*. 2016;6:1106-1117.
 33. Kytölä S, Vänttinen I, Ruokoranta T, et al. Ex vivo venetoclax sensitivity predicts clinical response in acute myeloid leukemia in the prospective VenEx trial. *Blood*. 2025;145:409-421.
 34. Kuusanmäki H, Kytölä S, Vänttinen I, et al. Ex vivo venetoclax sensitivity testing predicts treatment response in acute myeloid leukemia. *Haematologica*. 2023;108:1768-1781.
 35. Yadav B, Pemovska T, Szwajda A, et al. Quantitative scoring of differential drug sensitivity for individually optimized anticancer therapies. *Sci Rep*. 2014;4:5193.
 36. lanevski A, Timonen S, Kononov A, Aittokallio T, Giri AK. SynTox-Profiler: an interactive analysis of drug combination synergy, toxicity and efficacy. *PLoS Comput Biol*. 2020;16(2):e1007604.
 37. lanevski A, Giri AK, Aittokallio T. SynergyFinder 3.0: an interactive analysis and consensus interpretation of multi-drug synergies across multiple samples. *Nucleic Acids Res*. 2022;50:W739-W743.
 38. Yadav B, Wennerberg K, Aittokallio T, Tang J. Searching for drug synergy in complex dose-response landscapes using an interaction potency model. *Comput Struct Biotechnol J*. 2015;13:504-513.
 39. Lux S, Milsom MD. EVI1-mediated programming of normal and malignant hematopoiesis. *HemaSphere*. 2023;7(10):e959.
 40. Lichtman EI, Du H, Shou P, et al. Preclinical evaluation of B7-H3-specific chimeric antigen receptor T cells for the treatment of acute myeloid leukemia. *Clin Cancer Res*. 2021;27:3141-3153.
 41. Yang J, Chen M, Ye J, Ma H. Targeting PRAME for acute myeloid leukemia therapy. *Front Immunol*. 2024;15:1378277.
 42. Hänzelmann S, Castelo R, Guinney J. GSEA: gene set variation analysis for microarray and RNA-Seq data. *BMC Bioinformatics*. 2013;14(1):7.
 43. Liberzon A, Birger C, Thorvaldsdóttir H, Ghandi M, Mesirov JP, Tamayo P. The molecular signatures database hallmark gene set collection. *Cell Syst*. 2015;1(6):417-425.
 44. Liberzon A, Subramanian A, Pinchback R, Thorvaldsdóttir H, Tamayo P, Mesirov JP. Molecular Signatures Database (MSigDB) 3.0. *Bioinformatics*. 2011;27(12):1739-1740.
 45. van Galen P, Hovestadt V, Wadsworth IJ, et al. Single-cell RNA-Seq reveals AML hierarchies relevant to disease progression and immunity. *Cell*. 2019;176(6):1265-1281.e24.
 46. Ng SWK, Mitchell A, Kennedy JA, et al. A 17-gene stemness score for rapid determination of risk in acute leukaemia. *Nature*. 2016;540:433-437.
 47. Petersen SL, Wang L, Yalcin-Chin A, et al. Autocrine, TNF α signaling renders human cancer cells susceptible to smac-mimetic-induced apoptosis. *Cancer Cell*. 2007;12:445-456.
 48. Lueck SC, Russ AC, Botzenhardt U, et al. Smac mimetic induces cell death in a large proportion of primary acute myeloid leukemia samples, which correlates with defined molecular markers. *Oncotarget*. 2016;7:49539-49551.
 49. Quek L, Otto GW, Garnett C, et al. Genetically distinct leukemic stem cells in human CD34⁺ acute myeloid leukemia are arrested at a hemopoietic precursor-like stage. *J Exp Med*. 2016;213(8):1513-1535.
 50. Bonnet D, Dick JE. Human acute myeloid leukemia is organized as a hierarchy that originates from a primitive hematopoietic cell. *Nat Med*. 1997;3(7):730-737.
 51. Yang T, Kozopas KM, Craig RW. The intracellular distribution and pattern of expression of Mcl-1 overlap with, but are not identical to, those of Bcl-2. *J Cell Biol*. 1995;128:1173-1184.
 52. Teh TC, Nguyen NY, Moujalled DM, et al. Enhancing venetoclax activity in acute myeloid leukemia by co-targeting MCL1. *Leukemia*. 2018;32:303-312.
 53. Bazinet A, Loghavi S, Wei Y, et al. Erythroid-predominant myelodysplastic neoplasms exhibit a distinct genomic landscape with poor outcomes after venetoclax-based therapy. *Leukemia*. 2025;39(9):2256-2265.
 54. Zeng AGX, Bansal S, Jin L, et al. A cellular hierarchy framework for understanding heterogeneity and predicting drug response in acute myeloid leukemia. *Nat Med*. 2022;28(6):1212-1223.
 55. Lagadinou ED, Sach A, Callahan K, et al. BCL-2 inhibition targets oxidative phosphorylation and selectively eradicates quiescent human leukemia stem cells. *Cell Stem Cell*. 2013;12:329-341.
 56. Zeng AGX, Iacobucci I, Shah S, et al. Single-cell transcriptional atlas of human hematopoiesis reveals genetic and hierarchy-based determinants of aberrant AML differentiation. *Blood Cancer Discov*. 2025;6(4):307-324.
 57. Chromik J, Saffertal C, Serve H, Fulda S. Smac mimetic primes apoptosis-resistant acute myeloid leukaemia cells for cytarabine-induced cell death by triggering necroptosis. *Cancer Lett*. 2014;344:101-109.
 58. Bhatt S, Pioso MS, Olesinski EA, et al. Reduced mitochondrial apoptotic priming drives resistance to BH3 mimetics in acute myeloid leukemia. *Cancer Cell*. 2020;38(6):872-890.e6.
 59. Frey NV, Luger S, Mangan J, et al. A phase I study using single agent birinapant in patients with relapsed myelodysplastic syndrome and acute myelogenous leukemia. *Blood*. 2014;124:3758.

60. Infante JR, Dees EC, Olszanski AJ, et al. Phase I dose-escalation study of LCL161, an oral inhibitor of apoptosis proteins inhibitor, in patients with advanced solid tumors. *J Clin Oncol*. 2014;32:3103-3110.
61. Pemmaraju N, Carter BZ, Bose P, et al. Final results of a phase 2 clinical trial of LCL161, an oral SMAC mimetic for patients with myelofibrosis. *Blood Adv*. 2021;5:3163-3173.
62. Schoenwaelder SM, Jarman KE, Gardiner EE, et al. Bcl-xL-inhibitory BH3 mimetics can induce a transient thrombocytopenia that undermines the hemostatic function of platelets. *Blood*. 2011;118(6):1663-1674.
63. Roberts AW, Seymour JF, Brown JR, et al. Substantial susceptibility of chronic lymphocytic leukemia to BCL2 inhibition: results of a phase I study of navitoclax in patients with relapsed or refractory disease. *J Clin Oncol*. 2012;30(5):488-496.
64. Judd AS, Bawa B, Buck WR, et al. BCL-XL-targeting antibody-drug conjugates are active in preclinical models and mitigate on-mechanism toxicity of small-molecule inhibitors. *Sci Adv*. 2024;10(40):eado7120.
65. Khan S, Zhang X, Lv D, et al. A selective BCL-XL PROTAC degrader achieves safe and potent antitumor activity. *Nat Med*. 2019;25:1938-1947.
66. Wang Z, Ramage CL, Ma H, et al. Anti-leukemia combinatorial efficacy of ABBV155, a B7H3-BCL-XL inhibitor antibody-drug conjugate, in combination with venetoclax through BCL-XL/BIM and BCL-2/BIM complex dissociations. *Blood*. 2024;144:2760.
67. Jia Y, Han L, Ramage CL, et al. Co-targeting BCL-XL and BCL-2 by PROTAC 753B eliminates leukemia cells and enhances efficacy of chemotherapy by targeting senescent cells. *Haematologica*. 2023;108:2626-2638.